Geoscientific
Model Development
Discussions

Open Access

JULES-crop: a parametrisation of crops in the Joint UK Land Environment Simulator

T. Osborne[1], **J. Gornall**[2], **J. Hooker**[3], **K. Williams**[2], **A. Wiltshire**[2], **R. Betts**[2,4], **and T. Wheeler**[5]

[1]National Centre for Atmospheric Science, University of Reading, Reading, UK
[2]Hadley Centre, Met Office, Exeter, UK
[3]Joint Research Centre, Ispra, Italy
[4]College of Life and Environmental Sciences, University of Exeter, Exeter, UK
[5]Department of Agriculture, University of Reading, Reading, UK

Correspondence to: J. Gornall (jemma.gornall@metoffice.gov.uk)

GMDD

7, 6773–6809, 2014

JULES-crop

T. Osborne et al.

Title Page

Abstract	Introduction
Conclusions	References
Tables	Figures

◄◄ ►►

◄ ►

Back Close

Full Screen / Esc

Printer-friendly Version

Interactive Discussion

Abstract

Studies of climate change impacts on the terrestrial biosphere have been completed without recognition of the integrated nature of the biosphere. Improved assessment of the impacts of climate change on food and water security requires the development
5 and use of models not only representing each component but also their interactions. To meet this requirement the Joint UK Land Environment Simulator (JULES) land surface model has been modified to include a generic parametrisation of annual crops. The new model, JULES-crop, is described and evaluation at global and site levels for the four globally important crops; wheat, soy bean, maize and rice is presented. JULES-
10 crop demonstrates skill in simulating the inter-annual variations of yield for maize and soy bean at the global level, and for wheat for major spring wheat producing countries. The impact of the new parametrisation, compared to the standard configuration, on the simulation of surface heat fluxes is largely an alteration of the partitioning between latent and sensible heat fluxes during the later part of the growing season. Further
15 evaluation at the site level shows the model captures the seasonality of leaf area index and canopy height better than in standard JULES. However, this does not lead to an improvement in the simulation of sensible and latent heat fluxes. The performance of JULES-crop from both an earth system and crop yield model perspective is encouraging however, more effort is needed to develop the parameterisation of the model for
20 specific applications. Key future model developments identified include the specification of the yield gap to enable better representation of the spatial variability in yield.

1 Introduction

Understanding how climate variability and change will impact upon crop production systems is a research challenge of utmost importance to society. To date, studies of cli-
25 mate change impacts on the terrestrial biosphere have been completed without recognition of the integrated nature of the biosphere. Crop simulation models are widely

Title Page

Abstract | Introduction

Conclusions | References

Tables | Figures

◄ | ►

◄ | ►

Back | Close

Full Screen / Esc

Printer-friendly Version

Interactive Discussion

utilised as they incorporate many known effects of how changes in atmospheric conditions can impact upon crop growth, development and yield. However, they do not simulate the wider interactions of crops and the environment. For example, climate change will impact upon water resources which will in turn impact upon the water available
5 for irrigation of crops. Betts et al. (2013) used the Hadley Centre Earth System Model (HadGEM2-ES) to evaluate climate impacts on the terrestrial biosphere under a range of emission scenarios. By doing so they were able to assess several elements of the terrestrial system in a way that was fully integrated and consistent with the climate projections. However, they were only able to include natural systems as crops are not yet
10 included in the model. Including a representation of crops within land surface models will facilitate a more comprehensive, integrated and internally-consistent simulation of the impacts of climate change and variability on the full land system, accounting for interactions between different components and processes. This will ultimately enable improved projections of the impacts of climate change on food and water security, in-
15 cluding interactions between the two. There is increasing evidence that the cultivation of crops affects weather and climate on local scales. Crop-lands now occupy 12 % of the Earth's ice-free land surface and in several regions of the world are the dominant vegetation type on the land surface (e.g. mid-West USA, Indo-Gangetic Plain). This extensification of agriculture has altered the biophysical characteristics of the land
20 surface potentially altering regional climate. Therefore, there is reasoning to consider crops and climate as a truly coupled system and hence motivation to develop models which can fully represent the coupled feedbacks between them.

Efforts to simulate the environmental impacts on crop production is commonly thought to have begun in the 1960s at Wageningen (van Ittersum et al., 2003). Since
25 then crop modelling has grown and there are now many models available in the research and agronomic domains. Such models have been deployed both as decision support tools, and to research the impacts of climate change on future crop production. Recent advances in crop modelling include the application of crop models, traditionally developed at the field level, to cover the globe on a gridded basis (Deryng et al., 2011;

Osborne et al., 2013), and inter-comparison of many crop models in simulating the same crop and the same set of conditions (Asseng et al., 2013).

The investigation of how crop-lands affect weather and climate is much less mature. Initial expansion of crop-land area came at the expense of forests and the impact of this deforestation has received considerable research attention. However, crop-lands have also replaced more similar native grasslands. For example, McPherson et al. (2004) showed that the near-surface climate over the now intensively cultivated winter wheat belt in Oklahoma, USA, is significantly different to that over adjacent grasslands. McPherson et al. (2004) identify the differences in phenology between managed crop-lands and natural grasslands as the determinant of the differences.

The increase in understanding of how crop-lands might differentially impact the climate compared to natural vegetation has led to a recent surge in model development whereby land surface or global vegetation models have been extended to include explicit parametrisations of crops, in place of the use of grasslands as a surrogate (see review of Levis, 2010). Some developments have been motivated by improving the carbon and water budget of land surface modelling (Bondeau et al., 2007), others to include crop-lands in global or regional climate models to better represent their impact on the atmosphere (Lokupitiya et al., 2009; Chen and Xie, 2012; Levis et al., 2012), while others have been motivated to consistently simulate both yield and environmental impacts (Kucharik and Brye, 2003).

The aim of this model development was to develop a combined land surface and crop model capable of simulating both the impacts of climate variability on crop productivity, as well as the impact of crop-lands on the climate. To achieve this we have added a crop-specific parametrisation to the Joint UK Land Environment Land Surface land surface model (JULES). JULES is the land surface scheme of the UK Met Office Unified Model and the next generation UK Earth System Model (UKESM) and therefore, can be in time coupled to a state of the art climate model. A full description of JULES can be found in Best et al. (2011) and Clark et al. (2011). JULES does not currently include an explicit parametrisation of crops, instead over cropped regions the

C3 or C4 grass plant functional type are used. Previous work has included crops in the model. Osborne et al. (2007) included a crop parametrisation in MOSES (i.e. in the fully coupled land-surface – climate model) based on the groundnut version of the crop model GLAM. More recently, Van den Hoof et al. (2011) extended JULES to include a parametrisation of wheat based on the crop model SUCROS. Neither Osborne et al. (2007) nor Van den Hoof et al. (2011) developed a generic representation of crops suitable for the examination of different crops throughout the globe something that is important from an Earth System Modelling perspective. Therefore, the objective of this study was to develop a generic parametrisation of crops applicable to many crop types and at the global scale. However, the model has been designed to be flexible meaning users can re-parametrize the model depending on requirements (e.g. to represent different crop cultivars).

The following Section describes the model development, Sects. 3 and 4 present evaluation of the new model when applied at global and site levels, respectively, followed by a Discussion (Sect. 5).

2 Model description

The essence of JULES-crop is illustrated in Fig. 1. The additional model equations required to simulate crops essentially partition the carbon uptake of vegetation already simulated by JULES in to several crop organs and the size of the crop, important for land surface-atmosphere feedbacks, is derived from the organ biomass using allometric equations. The pattern of partitioning of assimilated carbon to the crop organs is affected by the crop development rate which itself is influenced by temperature. In addition to the new equations describing crop growth and development, changes to the model structure were also required to accommodate the additional plant functional types. New equations describing crop growth and development were added to the model. Each crop is considered as an additional plant functional type and a distinction is made between natural and crop plant functional types within the model, with the

Back | Close

Full Screen / Esc

Printer-friendly Version

Interactive Discussion

crop plant functional types requiring extra parameters to be specified. The detailed description of the crop parametrisation is split in to three parts. Firstly, the equations that determine the start and duration of the crop *growing season* are described. Secondly, the equations determining the rate of crop *growth* are described. Lastly, the changes to model structure are outlined. A full listing of new model parameters and variables can be found in Tables 1 and 2, respectively.

2.1 Growing season and development

The crop growing season begins when the crop is sown. This date can either be prescribed (i.e. if it is know) or calculated dynamically based on environmental criteria. In the latter case, sowing only occurs when the soil is wet enough ($\theta_2 > \theta_{c,2}$, where θ_2 is the soil moisture content in the second layer and $\theta_{c,2}$ is the critical soil moisture content in the second layer), it is warm enough ($T_{soil,3} > T_b + 2\,\mathrm{K}$, where $T_{soil,3}$ is the temperature in the third soil layer and T_b is the base temperature), and days are not rapidly shortening ($\mathrm{d}P/\mathrm{d}t > -0.02$ hours per day, where P is the day length). The use of sub-surface soil moisture and temperature variables prevents sowing occurring too early in response to short term fluctuations in weather. The rate of day length criteria ensures that crops are not sown too late in the year when conditions for growth are deteriorating.

Once sown, the crop develops through three stages: sowing to emergence, emergence to flowering, and flowering to maturity. Harvest is assumed to occur at crop maturity. The rate of crop development is related to thermal time. Given the 1.5 m tile temperature (T), an effective temperature (T_{eff}) is calculated based upon the crop-specific

Title Page

Abstract | Introduction

Conclusions | References

Tables | Figures

|◄ | ►|

◄ | ►

Back | Close

Full Screen / Esc

Printer-friendly Version

Interactive Discussion

cardinal temperatures (T_b, T_o, T_m).

$$
T_{eff} = \begin{cases}
0 & \text{for} \quad T < T_b \\
T - T_b & \text{for} \quad T_b \leq T \leq T_o \\
(T_o - T_b)\left(1 - \dfrac{T - T_o}{T_m - T_o}\right) & \text{for} \quad T_o < T < T_m \\
0 & \text{for} \quad T \geq T_m
\end{cases} \tag{1}
$$

T_{eff} is greatest, and hence development fastest, at $T = T_o$. As temperature falls below, or rises above T_o the rate of development linearly decreases until no development occurs when either $T \leq T_b$ or $T \geq T_m$. For the sowing to emergence phase, T_{eff} is not affected by T_m or T_o (i.e. $T_{eff} = T - T_b$).

For some crops, progress towards flowering is slowed if the day length (P) is less than (greater than) a crop-specific critical photoperiod (P_{crit}) for long-day (short-day) crop types. The degree of sensitivity to photoperiod is represented by the parameter P_{sens} which is positive for short-day plants and negative for long-day plants. Therefore, to slow development T_{eff} is multiplied by the relative photoperiod effect (RPE), which is defined as follows:

$$
\text{RPE} = 1 - (P - P_{crit})P_{sens} \tag{2}
$$

The status of crop development is represented by the Development Index (DVI) which takes the value of -1 upon sowing, increasing to 0 on emergence, 1 at the end of vegetative stage and 2 at crop maturity. The rate of increase of DVI is calculated as follows:

$$
\frac{d\text{DVI}}{dt} = \begin{cases}
\dfrac{T_{eff}}{\text{TT}_{emr}} & \text{for} \quad -1 \leq \text{DVI} < 0 \\[2mm]
\left(\dfrac{T_{eff}}{\text{TT}_{veg}}\right)\text{RPE} & \text{for} \quad 0 \leq \text{DVI} < 1 \\[2mm]
\dfrac{T_{eff}}{\text{TT}_{rep}} & \text{for} \quad 1 \leq \text{DVI} < 2
\end{cases} \tag{3}
$$

The growing season ends when DVI = 2 at which time the prognostic variables related to crop growth ($L, h, C_{root}, C_{harv}, C_{resv}$) are reset to minimal values close to zero. To prevent growing seasons continuing indefinitely when conditions are no longer suitable the crop is also harvested if the soil temperature in the second soil layer falls below T_b

5 at any time after DVI = 1 or if LAI > 15. Vernalisation, a cold temperature requirement for development in some crops, is not included in this model version.

2.2 Growth

To simulate crop growth, Net Primary Productivity (Π) is accumulated over a day and then partitioned between five carbon pools: root (C_{root}), structural stem (C_{stem}), stem

10 reserves (C_{resv}), leaves (C_{leaf}), and harvested organs (C_{harv}). The original formulation for Π in JULES includes assumptions about the sizes of the leaf, stem and root carbon pools in order to estimate respiration loses. Stem carbon is a function of leaf area index (Eq. 46 of Clark et al., 2011) and root carbon is set to equal leaf carbon. Because these carbon pools are now explicitly simulated, Π is recalculated for the crop types

15 the following equation based on an algebraic reduction of the set of equations used in JULES:

$$\Pi = 0.012 \left(1 - r_g\right) \left(A_c - R_{dc} \left(\frac{C_{root} + C_{stem}}{C_{leaf}}\right)\right) \tag{4}$$

where r_g is the fraction of Gross Primary Productivity less maintenance respiration that

20 is assigned to growth respiration, A_c is the net canopy photosynthesis, and R_{dc} is the rate of non-moisture stressed canopy dark respiration. C_{leaf}, C_{stem} and C_{root} are the carbon content of leaf, stem and root, respectively.

The carbon in Π is accumulated over a day and then divided into five crop components according to "partition coefficients", one for each of the four root, stem, leaf and

25 harvest pools defined above and a reserve pool. These components are added to the

(state variable) pools of carbon describing the crop.

$$\frac{dC_{root}}{dt} = p_{root}\Pi$$

$$\frac{dC_{leaf}}{dt} = p_{leaf}\Pi$$

$$\frac{dC_{stem}}{dt} = p_{stem}\Pi(1 - \tau)$$

$$\frac{dC_{harv}}{dt} = p_{harv}\Pi$$

$$\frac{dC_{resv}}{dt} = p_{stem}\Pi\tau \tag{5}$$

where τ is the fraction of stem carbon that is partitioned in to the reserve pool. $p_{root} + p_{leaf} + p_{stem} + p_{harv} = 1.0$.

Partition coefficients for a given crop are typically pre-defined in process-based crop models according to either the length of time since emergence, or to crop development stage (DVI, i.e. a function of thermal time since emergence). They are represented by fixed values for a given period of time (or thermal time) since emergence, and these values are listed in a look-up table and referenced for each iteration of the model (e.g. WOFOST, van Ittersum et al., 2003). But how much detail is required to describe the evolution of partition coefficients through the growing crop's duration? Say, for example, that only 2 values are wanted (to define the partition coefficient during vegetative and reproductive periods), and that there are 4 carbon pools, then we would need $2 + (4 - 1) = 6$ partition coefficients (partition coefficients are only needed for 3 of the 4 pools, as the fourth is defined as 1 minus the sum of the other 3). If more detail in the evolution of the partition coefficients is desired, then more values are required at finer temporal (or thermal temporal) resolution. This can lead to very many partition coefficients being defined and used. Instead, we define the partition coefficients as a function of thermal time. Thus, for only 6 parameters defining this functional form, we

can describe continuously varying partition coefficients over the duration of the crop cycle. We use a multinomial logistic to define this function:

$$p_{\text{root}} = \frac{e^{\alpha_{\text{root}}+(\beta_{\text{root}}\text{DVI})}}{e^{\alpha_{\text{root}}+(\beta_{\text{root}}\text{DVI})} + e^{\alpha_{\text{stem}}+(\beta_{\text{stem}}\text{DVI})} + e^{\alpha_{\text{leaf}}+(\beta_{\text{leaf}}\text{DVI})} + 1}$$

$$p_{\text{stem}} = \frac{e^{\alpha_{\text{stem}}+(\beta_{\text{stem}}\text{DVI})}}{e^{\alpha_{\text{root}}+(\beta_{\text{root}}\text{DVI})} + e^{\alpha_{\text{stem}}+(\beta_{\text{stem}}\text{DVI})} + e^{\alpha_{\text{leaf}}+(\beta_{\text{leaf}}\text{DVI})} + 1}$$

$$p_{\text{leaf}} = \frac{e^{\alpha_{\text{leaf}}+(\beta_{\text{leaf}}\text{DVI})}}{e^{\alpha_{\text{root}}+(\beta_{\text{root}}\text{DVI})} + e^{\alpha_{\text{stem}}+(\beta_{\text{stem}}\text{DVI})} + e^{\alpha_{\text{leaf}}+(\beta_{\text{leaf}}\text{DVI})} + 1}$$

$$p_{\text{harv}} = \frac{1}{e^{\alpha_{\text{root}}+(\beta_{\text{root}}\text{DVI})} + e^{\alpha_{\text{stem}}+(\beta_{\text{stem}}\text{DVI})} + e^{\alpha_{\text{leaf}}+(\beta_{\text{leaf}}\text{DVI})} + 1} \tag{6}$$

where α and β are empirically derived parameters describing the shape of the thermal time varying partition coefficient for leaves, roots and stems, and DVI is the development index. Thus for only six parameters (which is also the absolute minimum number of parameters needed to define partition coefficients for four carbon pools with only values for vegetative and reproductive periods, as, obviously, harvested components cannot be added to before flowering!) we can define a much wider range of shapes of thermal time varying partition coefficients. What's more, these six parameters can be more feasibly calibrated than a larger number of 'look-up' partition coefficients. This parametrisation is illustrated in Fig. 2 overlaid with example observed partitioning fractions from de Vries et al. (1989).

Following the formulation of de Vries et al. (1989), once carbon is no longer partitioned to stems, carbon from the stem reserve pool is mobilised to the harvest pool at a rate of 10 % a day:

$$\left.\begin{array}{l} C_{\text{harv}} = C_{\text{harv}} + (0.1 C_{\text{resv}}) \\ C_{\text{resv}} = 0.9 C_{\text{resv}} \end{array}\right\} \quad \text{for} \quad p_{\text{stem}} < 0.01. \tag{7}$$

Leaf senescence is treated simplistically by mobilising carbon from the leaf to the harvest pool at a rate of $0.05 d^{-1}$ once DVI has reached 1.5:

$$\left.\begin{array}{l} C_{\text{harv}} = C_{\text{harv}} + (0.05 C_{\text{leaf}}) \\ C_{\text{leaf}} = 0.95 C_{\text{leaf}} \end{array}\right\} \quad \text{for} \quad \text{DVI} > 1.5. \tag{8}$$

5   At the end of each growth time step (24 h), the amount of carbon in the leaves is related to leaf area index (L) by:

$$L = \frac{C_{\text{leaf}}}{f_C} \text{SLA} \tag{9}$$

where

10   $$\text{SLA} = \gamma \left(\text{DVI} + 0.06\right)^{\delta} \tag{10}$$

The values of γ and δ were determined by fitting the relationship to the paired values of DVI and SLA reported in de Vries et al. (1989).

The amount of carbon in the stem is related to the crop height by:

15   $$h = \kappa \left(\frac{C_{\text{stem}}}{f_C}\right)^{\lambda} \tag{11}$$

The values of κ and λ were determined by fitting the relationship to the paired values of h and C_{stem} at the Mead FLUXNET site (Verma et al., 2005).

Equations (9) and (11) are rearranged to derive the carbon content of leaves and
20   stems, respectively, before each growth time step.

Because root biomass increases during the crop growing season the fraction of roots in each JULES soil layer varies according to the equation of Arora and Boer (2003) which defines the fraction of roots at depth z as:

25   $$f = 1 - e^{-\frac{z}{a}} \tag{12}$$

where

$$a = d_r \left(\frac{C_{\text{root}}}{f_C} \right)^{r_{\text{dir}}} \tag{13}$$

where d_r is 0.5 for all crop types, and r_{dir} is a crop-specific parameter.

To ensure crop establishment, the growing season is curtailed if the sum of root, leaf, stem and reserve carbon falls below the initial seed carbon content (or zero) if the sowing date is being determined dynamically.

2.3 Changes to JULES code structure

The standard version of JULES represents the land surface as a combination of up to 9 surface types: broad-leaf trees, needle-leaf trees, C3 grass, C4 grass, shrubs, bare-soil, inland lakes, snow and ice. Surface fluxes of heat, moisture and momentum are determined independently for each tile before being combined to a single set of fluxes according to the relative fractions of each tile. Each crop type is considered as a different tile. Therefore, it is possible to simulate many crops or crop types at a site or grid box in a single integration of JULES, in addition to the standard five plant functional types. The parameters required to represent vegetation within JULES were extended to the crop tile(s). The values were copied across from the JULES default parameters for C3 and C4 grass, depending on the crop photosynthetic capacity (see Table 3).

The values of the parameters required in Eqs. (1)–(13) determine which crop (e.g. maize or wheat), crop type (e.g. C3 cereals or tropical oilseed) or cultivar (e.g. Soy bean PS123121 or Soy bean 21h321) are being simulated. Each parameter is described in Table 1. Values for each parameter can determined by calibration against relevant observational data such as leaf area index, biomass, yield from agricultural field stations. For this study such an exercise was not performed. Instead, suitable values were determined from either the literature or by tuning to fit site level data in order to establish a model version that could be evaluated at site and global scales.

3 Global simulation

3.1 Model set-up

To evaluate the potential of JULES-crop as a global gridded crop, model simulations for the period 1960 to 2010 were performed over the global domain. Four crop types were simulated; wheat, soy bean, maize and rice. Parameter values are in Table 4 and were either taken from the crop science literature or tuned. Specifically, the values for the partition parameters $\alpha_{\text{root,stem,leaf}}$ and $\beta_{\text{root,stem,leaf}}$ and the specific leaf area coefficients γ and δ were calibrated against data in de Vries et al. (1989). The allometric coefficients κ and λ were determined by calibration against paired crop height and stem biomass data from FLUXNET sites. The cardinal temperatures (T_{b}, T_{o}, and T_{m}) were specified values widely used in the literature. The effect of photoperiod was not included (by setting P_{crit} to 24) due to our method of determining TT_{veg} and TT_{rep} (see below). The parameter r_{dir} was set to zero for all crop types which effectively removes the effect of increasing root carbon on the vertical distribution. Early tests of the model revealed that including an effect of increasing root carbon led to high levels of water stress at the start of the crop growing season leading to poor crop growth. Therefore, the effect was "turned-off". The parametrisation was left in the model to allow other model users to experiment further with dynamic root growth.

he global model runs were driven by the CRU-NCEPv4 climate data extended to include 2012 (N. Viovy, personal communication, 2013) as used by the Global Carbon Project (Le Quéré et al., 2013). This was regridded to a n96 grid and used with ancillaries from HadGEM2-ES (Collins et al., 2011; Jones et al., 2011) to evaluate the performance of the model in a Earth System Model set-up. A multi-layer canopy radiation scheme was used, accounting for direct/diffuse radiation components including sun-flecks (can_ran_mod = 5). The main run was from 1960 to 2010 and the spin up consisted of repeating the first ten years five times. The sowing dates were taken from Sacks et al. (2010), and a value for each land gridbox obtained using nearest-neighbour extrapolation. The values of TT_{veg} and TT_{rep} were allowed to vary spatially

and determined such that, when used with the CRU-NCEP temperature climatology 1990–2000 and the Sacks et al. (2010) sowing date, the crop reached DVI = 2.0 at the Sacks et al. (2010) harvesting dates, with $x = \mathrm{TT_{veg}}/(\mathrm{TT_{veg}} + \mathrm{TT_{rep}}) = 0.5, 0.45, 0.6, 0.6$ for soy bean, maize, wheat, rice respectively. Photoperiod sensitivity was not consid-
5 ered. For comparison a control run was completed using the same model set-up but with the crop code switched off. This run is used to assess performance against the standard land surface scheme in the Met Office Hadley Centre Earth System Model – HadGEM2-ES.

Figure 3 shows the planting date of Sacks et al. (2010) and the derived maps of $\mathrm{TT_{veg}}$
10 and $\mathrm{TT_{rep}}$. Sacks et al. (2010) derived gridded planting dates from national or district level reported planting dates which are given in months rather than days. Therefore, there is little spatial or temporal variation in the sowing date which might well be expected due to variations in local climate and management practices. However, the data serves a purpose in global modelling studies by providing an approximate start point for
15 the growing season an the right time of year. Our method of calculating the crop thermal time requirements produces considerable spatial variability which is determined in reality by variation in the choice of crop cultivar chosen. Other global crop modelling studies have approached the issue of specifying these requirements at the global scale in different ways. Osborne et al. (2013) chose three sets of thermal time requirements
20 and applied them over the globe allowing for assessment of which were most suitable after the simulations, whereas Deryng et al. (2011) related thermal time requirements (calculated from Sacks et al. (2010) in a similar manner to this study) to the annual accumulated thermal time and then used that relationship to determine thermal time requirements under future climate. The approach in this study was chosen as the sim-
25 plest and most likely to achieve growing seasons of lengths close to observed. Due to the absence of a vernalisation parametrisation in the model only spring wheat was considered. The crop fractions were taken from Monfreda et al. (2008) and re-gridded to the n96 HadGEM2-ES resolution. Monfreda et al. (2008) provide observations in the

year 2000 which were used to described the crop coverages for the whole integration period due to a lack of available data sets covering this time period.

3.2 Evaluation

The grid box annual yield for each crop averaged over the 50 years is shown in Fig. 4. Typically, the lowest yields are simulated in arid regions which is unsurprising given the lack of any irrigation in the current model. For wheat the highest yields are simulated in the mid-latitudes whilst for maize and rice the highest yields are simulated in the Tropics. Given that the model does not include any information on the yield gap (the difference between actual farm level yield and potential yield) the spatial variability of model output should not be too closely compared to that of observed yield. Instead, a greater appreciation of model performance can be gained from examining the year to year fluctuations in yield, given that the effects of changes in management and technology materialise over several years.

Figures 5 shows the simulated global yield for wheat, soy bean, maize and rice between 1960–2008 compared to the reported yields of FAO (2014). Simulated global yield was determined by multiplying the simulated annual maximum yield at each grid cell by the observed harvested area from Monfreda et al. (2008) regridded to the HadGEM2-ES spatial resolution. This grid cell estimate of production was summed over all grid cells to produce an estimate of global production which was then divided by the total harvested area to provide an estimate of global yield. Grid cell yields were determined from the annual maximum value of C_{harv} which was multiplied by 2 to convert from carbon mass to total biomass, by 1.16 to account for grain moisture content, and by 10 to convert from $kg\,m^{-2}$ to $Mg\,ha^{-1}$. Not all grid cells were included in the analysis. Cells were excluded if the annual maximum DVI was less than 1.5 which was possible if the growing season was curtailed if LAI > 15 or $t_{soil,2} < T_{bse}$.

The average simulated yield level for wheat is similar to the most recent observations but when comparing the year to year fluctuations in yield, the correlation between simulated and observed is low ($r = 0.03$).Because JULES-crop only simulates spring

wheat then the comparison to reported wheat yields is slightly unfair given that the majority of wheat produced globally is from winter varieties. It is encouraging that the best agreement between simulated and observed yield fluctuations at the national level is for Turkey ($r = 0.46$) and Australia ($r = 0.56$), in which spring wheat varieties dominate.

5   For soy bean, average yield is much greater then observed but year on year variability is correlated with observations ($r = 0.39$) providing some confidence in the model's ability to simulate the observed response of soy bean yield to climate. The simulated variability is much greater than observed. Similarly for maize, variability is over estimated but does vary in line with observations ($r = 0.50$).For rice, yield levels are

10   higher than reported, variability is overestimated and not correlated with observations ($r = 0.16$). The tendency for JULES-crop to simulate larger variability than observed may in part be explained by the lack of any representation of irrigation in the model which would act to reduce the extent of crop failure in drought years. It may also be a result of the source-driven nature of the model. By relying on assimilated carbon

15   to increase crop size leading to greater growth, slight deviations in early growth can have potentially large consequences for future growth. In contrast, sink-driven models increase crop size before determining biomass growth and are therefore less sensitive to sub-optimal environmental conditions during the start of the growing season.

        To evaluate the impact of including the crop parametrisation on JULES, output from

20   the simulation with crops included is compared to a control simulation of the standard JULES configuration with grass plant functional types taking the land fraction of crops. Impacts on the land surface will be mostly mediated via direct changes to the vegetation structure and also via indirect effects on state variables, most obviously the soil moisture content. To begin to examine the potential for impact, the changes to a key

25   vegetation variable (LAI) are shown in Fig. 6 for four major crop producing countries. To produce the country averages, grid cell LAI are combined by weighting by the grid cell contribution to total country crop area. In the USA and China each crop growing season occupies the similar set of Summer months, where as for India and Brazil the wheat cropping season is distinct from the other three crops. Peak LAI is greatest in

Brazil and lowest in China which is most likely a reflection of the absence of irrigation in the model and the relative abundance of rainfall in each country. In comparison to the standard JULES configuration the addition of crops adds a seasonality to LAI as there is no default seasonality to vegetation characteristics in JULES. The annual variation of crop LAI is dampened when aggregated with the other plant functional types which explains the non-zero LAI in the non-growing season in the JULES-crop simulation.

Figure 7 shows that the impact of these differences in vegetation size during the year is greatest for the surface moisture flux and sensible heat flux rather than the components of the radiation balance. The largest impacts are on the sensible heat flux towards the end of the crop growing season when the heat flux is higher with the inclusion of crops. For India there is a concomitant decrease in the surface moisture flux implying that the total available energy at the surface is unaltered but is partitioned differently between sensible and latent heat fluxes.

4 Site simulation

4.1 Model set-up

To further understand the impact of adding crops to JULES, site level simulations were also performed. Evaluation was restricted to sites at which crops were grown and with availability of suitable meteorological data to drive the model and biological and flux data for evaluation. The sites selected were are all in the USA; Mead in Nebraska (Verma et al., 2005), and Bondville and Fermi, Illinois. For each site three simulations were performed; the standard configuration of JULES, standard JULES with the existing phenology parametrisation turned on, and the full JULES-crop parametrisation. For the JULES-crop simulation the fractional coverage of the relevant crop type was set to 1 with all other functional types set to 0. For the JULES (non-crop) simulations, the fractional coverage of the relevant grass functional type (i.e. C3 grass for soy bean, C4 for maize) was set to 1. All crop parameters were prescribed the same value as in the

global simulations. The sowing date, and thermal time requirements were taken from the relevant grid cell for each site.

4.2 Evaluation

Figure 8 compares JULES-crop simulations for the soy bean crop type with standard JULES C3 grass plant functional type with and without phenology, and with observations where available, in 2002 and 2004 at the Mead FLUXNET site. The crop parametrisation captures the evolution of leaf area index and crop height with different success in each year. In 2004 JULES-crop simulates the observed peak LAI well whereas in 2002 the simulated LAI is lower than observed. In both years the crop height is lower than observed. The standard C3 grass with phenology configuration of JULES also simulates growth and decay of vegetation cover but over a longer period of time than the observed growing season. Without the phenology routine the LAI is set to the default for C3 grass of 2.0 all year. Interestingly, the more realistic simulation of vegetation cover does not lead to improved simulation of surface fluxes. In both years similar characteristics of the simulations are evident. During winter all three configurations simulate similar fluxes in line with observations. Towards the start of the growing season the standard configuration of JULES with constant LAI = 2.0 over estimates latent heat flux due to an unrealistically large vegetation coverage. The simulations with phenology and crops have lower vegetation cover and simulate lower latent heat flux but are still noticeably greater than observations. At around the peak of crop cover all simulations underestimate the latent heat flux and over estimate the sensible heat flux.

Site level simulations for the maize crop type are shown in Fig. 9. At Bondville in 2001 the crop simulation slightly underestimates the peak LAI observed leading to slightly lower latent heat flux than observed. Overall, model simulations broadly capture the patterns of observed LAI, canopy height and latent and sensible heat fluxes although again there are no major improvements in model performace with the explicit inclusion of crops. At Fermi in 2006 the crop specific simulation captures the observed evolution of LAI reasonably well with excessive LAI slightly closer to observations than the

standard JULES simulations. This again does not improve the simulation of heat fluxes. All model configurations overestimate the partitioning of energy in to latent heat before the growing season begins and underestimate it during the crop growing season, despite widely varying LAI values. This comparison therefore serves as a reminder that improving the realism of a model does not guarantee improved performance in the model in other aspects. However, it is also worth noting that the parameters used for the crop model in the site simulations are from the global set-up and hence may not be optimal.

5 Discussion and Conclusions

When designing JULES-crop we took a flexible approach in acknowledgement of the different requirements of the science community. This means the model can be used to address a range of science questions for example (a) to assess global climate impacts on crop functional types over long integrations with climate model output, (b) to represent a number of crop cultivars of the same crop type at the site scale forced with weather observations and (c) to assess how crops may impact on biogeochemical feedbacks to climate including albedo, partitioning of turbulent fluxes and seasonality of LAI. In this paper we present results from a generic, crop functional type parametrization implemented at both global and site scale to show how this model performs in an Earth System Model context. Having the aim of generality necessarily means that the model loses out in terms of specificity. However, with further effort it should be possible to tailor the model set-up for more specific applications but with the requirement that attention is given to the choice of parameter values. Default values are provided here as a starting point for model development and initial evaluation.

These results demonstrate the importance of evaluating the performance of JULES-crop in a holistic sense, assessing both its ability to simulate land surface fluxes in addition to crop growth and development dynamics and to recognise that identified biases in performance are the result of the combined JULES-crop model, not just the

added crop component. Adding a crop parametrisation has increased the complexity of JULES. However, this has not led to an immediate improvement in the model's simulation of surface fluxes, at least at the measurement sites examined. More effort needs to go into developing the parameter sets for crops within JULES particularly the existing set of plant functional type parameters which control productivity.

As a yield simulation model, there are encouraging signs that JULES-crop can simulate variability in yield associated with climate fluctuations. However, it is clear that JULES-crop overestimates the magnitude of this variability. The global runs show that the model under-predicts yield in arid regions which highlights the importance of including irrigation in the near future. Whilst the absence of irrigation is most likely a contributing factor to the over-estimation of yield variability, the implication that the model is too sensitive to changes in environmental conditions should also be investigated further.

Crop production systems are by their very nature heavily influenced by humans. This represents a challenge to the JULES model which, to date, assumed vegetation to be static and, within each vegetation tile, homogeneous by the use of global constants for parameter values. The level to which this approach can be extended to crops is limited. Whilst some processes might be considered fundamental (i.e. photosynthesis) others can vary from place to place for the same crop (e.g. sensitivity of development rate to day length). Further still, human interference can alter the fundamental process, for example the application of fertiliser to increase leaf nitrogen contents impacting on photosynthesis. For applications of JULES-crop that rely on accurate yield simulations the inclusion of either a yield gap variable, or the factors that determine it such as fertilizer applications, pest control, soil fertility, should be a priority for future model development.

Title Page

Abstract | Introduction

Conclusions | References

Tables | Figures

◄ | ►

◄ | ►

Back | Close

Full Screen / Esc

Printer-friendly Version

Interactive Discussion

References

Arora, V. and Boer, G.: A representation of variable root distribution in dynamic vegetation models, Earth Interact., 7, 1–19, 2003. 6783

Asseng, S., Ewert, F., Rosenzweig, C., Jones, J. W., Hatfield, J. L., Ruane, A. C., Boote, K. J., Thorburn, P. J., Rötter, R. P., Cammarano, D., Brisson, N., Basso, B., Martre, P., Aggarwal, P. K., Angulo, C., Bertuzzi, P., Biernath, C., Challinor, A. J., Doltra, J., Gayler, S., Goldberg, R., Grant, R., Heng, L., Hooker, J., Hunt, L. A., Ingwersen, J., Izaurralde, R. C., Kersebaum, K. C., Müller, C., Kumar, S. N., Nendel, C., O'Leary, G., Olesen, J. E., Osborne, T. M., Palosuo, T., Priesack, E., Ripoche, D., Semenov, M. A., Shcherbak, I., Stedutoand, P., Stöckle, C., Stratonovitch, P., Streck, T., Supit, I., Tao, F., Travasso, M., Waha, K., Wallach, D., White, J. W., Williams, J. R., and Wolf, J.: Uncertainty in simulating wheat yields under climate change, Nature Clim. Change, 3, 827–832, 2013. 6776

Best, M. J., Pryor, M., Clark, D. B., Rooney, G. G., Essery, R .L. H., Ménard, C. B., Edwards, J. M., Hendry, M. A., Porson, A., Gedney, N., Mercado, L. M., Sitch, S., Blyth, E., Boucher, O., Cox, P. M., Grimmond, C. S. B., and Harding, R. J.: The Joint UK Land Environment Simulator (JULES), model description – Part 1: Energy and water fluxes, Geosci. Model Dev., 4, 677–699, doi:10.5194/gmd-4-677-2011, 2011. 6776

Betts, R. A., Golding, N., Gonzalez, P., Gornall, J., Kahana, R., Kay, G., Mitchell, L., and Wiltshire, A.: Climate and land use change impacts on global terrestrial ecosystems, fire, and river flows in the HadGEM2-ES Earth System Model using the Representative Concentration Pathways, Biogeosciences Discuss., 10, 6171–6223, doi:10.5194/bgd-10-6171-2013, 2013. 6775

Bondeau, A., Smith, P., Zaehle, S., Schaphoff, S., Lucht, W., Cramer, W., Gerten, D., Lotze-Campen, H., Müller, C., Reichstein, M., and Smith, B.: Modelling the role of agriculture for the 20th century global terrestrial carbon balance, Glob. Change Biol., 13, 679–706, 2007. 6776

Chen, F. and Xie, Z.: Effects of crop growth and development on regional climate: a case study over East Asian monsoon area, Clim. Dynam., 38, 2291–2305, 2012. 6776

Clark, D. B., Mercado, L. M., Sitch, S., Jones, C. D., Gedney, N., Best, M. J., Pryor, M., Rooney, G. G., Essery, R. L. H., Blyth, E., Boucher, O., Harding, R. J., Huntingford, C., and Cox, P. M.: The Joint UK Land Environment Simulator (JULES), model description – Part 2:

Carbon fluxes and vegetation dynamics, Geosci. Model Dev., 4, 701–722, doi:10.5194/gmd-4-701-2011, 2011. 6776, 6780

Collins, W. J., Bellouin, N., Doutriaux-Boucher, M., Gedney, N., Halloran, P., Hinton, T., Hughes, J., Jones, C. D., Joshi, M., Liddicoat, S., Martin, G., O'Connor, F., Rae, J., Senior, C., Sitch, S., Totterdell, I., Wiltshire, A., and Woodward, S.: Development and evaluation of an Earth-System model – HadGEM2, Geosci. Model Dev., 4, 1051–1075, doi:10.5194/gmd-4-1051-2011, 2011. 6785

de Vries, F. P., Jansen, D., ten Berge, H., and Bakema, A.: Simulation of ecophysiological processes of growth in several annual crops, p. 271, Pudoc Wageningen, 1989. 6782, 6783, 6785

Deryng, D., Sacks, W. J., Barford, C. C., and Ramankutty, N.: Simulating the effects of climate and agricultural management practices on global crop yield, Global Biogeochem. Cy., 25, GB2006, doi:10.1029/2009GB003765, 2011. 6775, 6786

FAO: FAOSTAT, available at: http://faostat.fao.org/, (last access: June 2014), 2014. 6787

Jones, C. D., Hughes, J. K., Bellouin, N., Hardiman, S. C., Jones, G. S., Knight, J., Liddicoat, S., O'Connor, F. M., Andres, R. J., Bell, C., Boo, K.-O., Bozzo, A., Butchart, N., Cadule, P., Corbin, K. D., Doutriaux-Boucher, M., Friedlingstein, P., Gornall, J., Gray, L., Halloran, P. R., Hurtt, G., Ingram, W. J., Lamarque, J.-F., Law, R. M., Meinshausen, M., Osprey, S., Palin, E. J., Parsons Chini, L., Raddatz, T., Sanderson, M. G., Sellar, A. A., Schurer, A., Valdes, P., Wood, N., Woodward, S., Yoshioka, M., and Zerroukat, M.: The HadGEM2-ES implementation of CMIP5 centennial simulations, Geosci. Model Dev., 4, 543–570, doi:10.5194/gmd-4-543-2011, 2011. 6785

Kucharik, C. and Brye, K.: Integrated BIosphere Simulator (IBIS) yield and nitrate loss predictions for Wisconsin maize receiving varied amounts of nitrogen fertilizer, J. Environ. Qual., 32, 247–268, 2003. 6776

Le Quéré, C., Peters, G. P., Andres, R. J., Andrew, R. M., Boden, T. A., Ciais, P., Friedlingstein, P., Houghton, R. A., Marland, G., Moriarty, R., Sitch, S., Tans, P., Arneth, A., Arvanitis, A., Bakker, D. C. E., Bopp, L., Canadell, J. G., Chini, L. P., Doney, S. C., Harper, A., Harris, I., House, J. I., Jain, A. K., Jones, S. D., Kato, E., Keeling, R. F., Klein Goldewijk, K., Körtzinger, A., Koven, C., Lefèvre, N., Maignan, F., Omar, A., Ono, T., Park, G.-H., Pfeil, B., Poulter, B., Raupach, M. R., Regnier, P., Rödenbeck, C., Saito, S., Schwinger, J., Segschneider, J., Stocker, B. D., Takahashi, T., Tilbrook, B., van Heuven, S., Viovy, N., Wanninkhof, R.,

Title Page

Abstract | Introduction

Conclusions | References

Tables | Figures

|◄ | ►|

◄ | ►

Back | Close

Full Screen / Esc

Printer-friendly Version

Interactive Discussion

Wiltshire, A., and Zaehle, S.: Global carbon budget 2013, Earth Syst. Sci. Data, 6, 235–263, doi:10.5194/essd-6-235-2014, 2014. 6785

Levis, S.: Modeling vegetation and land use in models of the Earth System, Climate Change, 1, 840–856, 2010. 6776

Levis, S., Bonan, G., Kluzek, E., Thornton, P. E., Jones, A., Sacks, W. J., and Kucharik, C. J.: Interactive cop management in the Community Earth System Model (CESM1): seasonal influences on land-atmoshpere fluxes., J Climate, 25, 4839–4859, 2012. 6776

Lokupitiya, E., Denning, S., Paustian, K., Baker, I., Schaefer, K., Verma, S., Meyers, T., Bernacchi, C. J., Suyker, A., and Fischer, M.: Incorporation of crop phenology in Simple Biosphere Model (SiBcrop) to improve land-atmosphere carbon exchanges from croplands, Biogeosciences, 6, 969–986, doi:10.5194/bg-6-969-2009, 2009. 6776

McPherson, R., Stensrud, D., and Crawford, K. C.: The impact of Oklahoma's winter wheat belt on the mesoscale environment, Mon. Weather Rev., 132, 405–421, 2004. 6776

Monfreda, C., Ramankutyy, N., and Foley, J.: Farming the planet: 2. Geographic distribution of crop areas, yields, physiological types, and net primary production in the year 2000, Global Biogeochem. Cy., 22, GB1022, doi:10.1029/2007GB002947, 2008. 6786, 6787

Osborne, T., Lawrence, D., Challinor, A., Slingo, J., and Wheeler, T.: Development and assessment of a coupled crop-climate model, Glob. Change Biol., 13, 169–183, 2007. 6777

Osborne, T., Rose, G., and Wheeler, T.: Variation in the global-scale impacts of climate change on crop productivity due to climate model uncertainty and adaptation, Agr. Forest Meteorol., 170, 183–194, doi:10.1016/j.agrformet.2012.07.006, 2013. 6776, 6786

Sacks, W. J., Deryng, D., Foley, J. A., and Ramankutty, N.: Crop planting dates: an analysis of global patterns, Global Ecol. Biogeogr., 19, 607–620, doi:10.1111/j.1466-8238.2010.00551.x, 2010. 6785, 6786, 6803

Van den Hoof, C., Hanert, E., and Vidale, P.-L.: Simulating dynamic crop growth with an adapted land surface model JULES-SUCROS: model development and validation, Agr. Forest Meteorol., 151, 137–153, 2011. 6777

van Ittersum, M., Leffelaar, P., van Keulen, H., Kropff, M., Bastiaans, L., and Goudriaan, J.: On approaches and applications of the Wageningen crop models, Eur. J. Agron., 18, 201–234, doi:10.1016/S1161-0301(02)00106-5, 2003. 6775, 6781

Verma, S. B., Dobermann, A., Cassman, K. G., Walters, D. T., Knops, J. M., Arkebauer, T. J., Suyker, A. E., Burba, G. G., Amos, B., Yang, H., Ginting, D., Hubbard, K. G., Gitelson, A. A., and Walter-Shea, E. A.: Annual carbon dioxide exchange in ir-

Title Page

Abstract | Introduction

Conclusions | References

Tables | Figures

|◄ | ►|

◄ | ►

Back | Close

Full Screen / Esc

Printer-friendly Version

Interactive Discussion

rigated and rainfed maize-based agroecosystems, Agr. Forest Meteorol., 131, 77–96, doi:10.1016/j.agrformet.2005.05.003, 2005. 6783, 6789

JULES-crop

T. Osborne et al.

Title Page

Abstract | Introduction

Conclusions | References

Tables | Figures

◄ | ►

◄ | ►

Back | Close

Full Screen / Esc

Printer-friendly Version

Interactive Discussion

Table 1. Crop model parameters used in JULES-crop.

Parameter	Unit	Equation	Description
T_b	°C	Eq. (1)	Base temperature
T_o	°C	Eq. (1)	Optimum temperature
T_m	°C	Eq. (1)	Maximum temperature
TT_{emr}	°C d	Eq. (3)	Thermal time between sowing and emergence
TT_{veg}	°C d	Eq. (3)	Thermal time between emergence and flowering
TT_{rep}	°C d	Eq. (3)	Thermal time between flowering and maturity/harvest
P_{crit}	h	Eq. (2)	Critical photperiod
P_{sens}	h^{-1}	Eq. (2)	Sensitivity of development rate to photoperiod
r_{dir}	–	Eq. (13)	Coefficient determine relative growth of roots vertically and horizontally
α_{root}	–	Eq. (6)	Coefficient for determining partitioning
α_{stem}	–	Eq. (6)	As above
α_{leaf}	–	Eq. (6)	As above
β_{root}	–	Eq. (6)	As above
β_{stem}	–	Eq. (6)	As above
β_{leaf}	–	Eq. (6)	As above
γ	$m^2\,kg^{-1}$	Eq. (10)	Coefficient for determining specific leaf area
δ	–	Eq. (10)	As above
τ	–	Eq. (5)	Fraction of stem growth partitioned to C_{resv}
f_C	–	Eqs. (9), (11), (13)	Carbon fraction of dry matter
κ	–	Eq. (11)	Allometric coefficient which relates C_{stem} to h
λ	–	Eq. (11)	As above

Table 2. Crop model variables in JULES-crop.

Variable	Unit	Equation	Description
New variables			
T_{eff}	°C	Eqs. (1), (3)	Effective temperature
DVI	–	Eqs. (3), (6), (8), (10)	Development Index
C_{leaf}	kg C m^{-2}	Eqs. (4), (5), (8), (9)	Leaf carbon pool
C_{stem}	kg C m^{-2}	Eqs. (4), (5), (11)	Stem carbon pool
C_{root}	kg C m^{-2}	Eqs. (4), (5), (13)	Root carbon pool
C_{harv}	kg C m^{-2}	Eqs. (5), (7), (8)	Harvested organ carbon pool
C_{resv}	kg C m^{-2}	Eqs. (5), (7)	Stem reserve carbon pool
p_{leaf}	–	Eqs. (5), (6)	Fraction of NPP partitioned to C_{leaf}
p_{stem}	–	Eqs. (5), (6), (7)	Fraction of NPP partitioned to C_{stem}
p_{root}	–	Eqs. (5), (6)	Fraction of NPP partitioned to C_{root}
p_{harv}	–	Eqs. (5), (6)	Fraction of NPP partitioned to C_{harv}
P	h	Eq. (2)	Photoperiod (day length)
RPE	–	Eqs. (2), (3)	Relative Photoperiod Effect
Existing variables			
T	°C	Eq. (1)	1.5 m temperature on each tile
L	m^2 m^{-1}	Eq. (9)	Leaf area index
SLA	m^2 kg^{-1}	Eqs. (9), (10)	Specific Leaf Area
h	m	Eq. (11)	Canopy Height
Π	kg C m^{-2}	Eqs. (4), (5)	Net primary productivity
A_c	kg C m^{-2}	Eq. (4)	Net carbon assimilation
R_{dc}	kg C m^{-2}	Eq. (4)	Canopy dark respiration

Table 3. JULES plant functional type parameters extended to represent crop types wheat, soy bean, maize and rice.
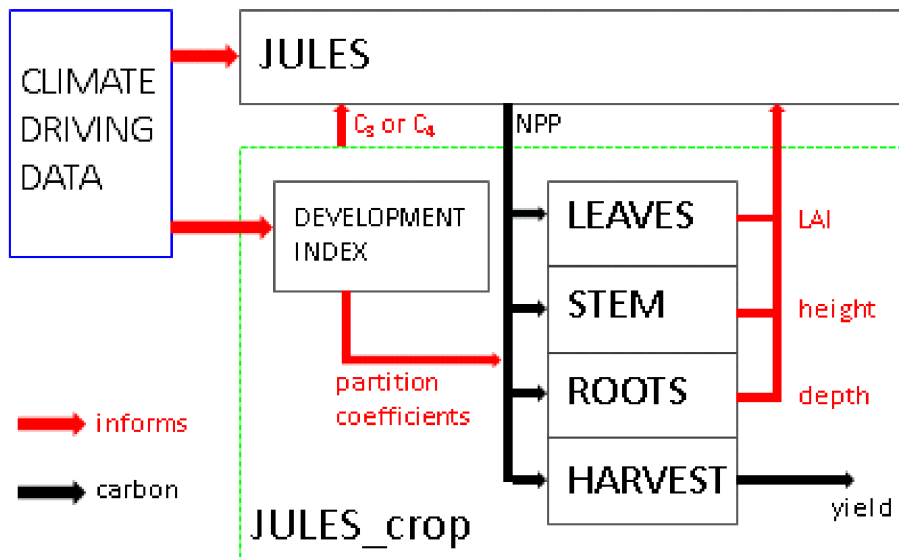
Crop type	Wheat	Soybean	Maize	Rice
$c3$	1	1	0	1
d_r	0.5	0.5	0.5	0.5
dq_{crit}	0.1	0.1	0.075	0.1
f_d	0.015	0.015	0.025	0.015
$f0$	0.9	0.9	0.8	0.9
n_{eff}	8.00×10^{-4}	8.00×10^{-4}	4.00×10^{-4}	8.00×10^{-4}
$n_l(0)$	0.073	0.073	0.06	0.073
σ_l	0.032	0.032	0.025	0.032
T_{low}	0	0	13	0
T_{upp}	36	36	45	36

Table 4. Parameter values used to represent crop types wheat, soy bean, maize and rice. See Table 1 for parameter definitions.

Crop type	Wheat	Soybean	Maize	Rice
T_b	0	5	8	8
T_o	20	27	30	30
T_m	30	40	42	42
TT_{emr}	35	35	80	60
TT_{veg}		See Fig. 3		
TT_{rep}		See Fig. 3		
P_{crit}	24	24	24	24
P_{sens}	0.00	0.00	0.00	0.00
r_{dir}	0.0	0.0	0.0	0.0
α_{root}	18.5	20.0	13.5	18.5
α_{stem}	16.0	18.5	12.5	19.0
α_{leaf}	18.0	19.5	13.0	19.5
β_{root}	−20.0	−16.5	−15.5	−19.0
β_{stem}	−15.0	−14.5	−12.5	−17.0
β_{leaf}	−18.5	−15.0	−14.0	−18.5
γ	27.3	25.9	22.5	20.9
δ	−0.0507	−0.1451	−0.2587	−0.2724
τ	0.40	0.18	0.35	0.25
f_C	0.5	0.5	0.5	0.5
κ	1.4	1.6	3.5	1.4
λ	0.4	0.4	0.4	0.4

Title Page

Abstract · Introduction

Conclusions · References

Tables · Figures

|◄ · ►|

◄ · ►

Back · Close

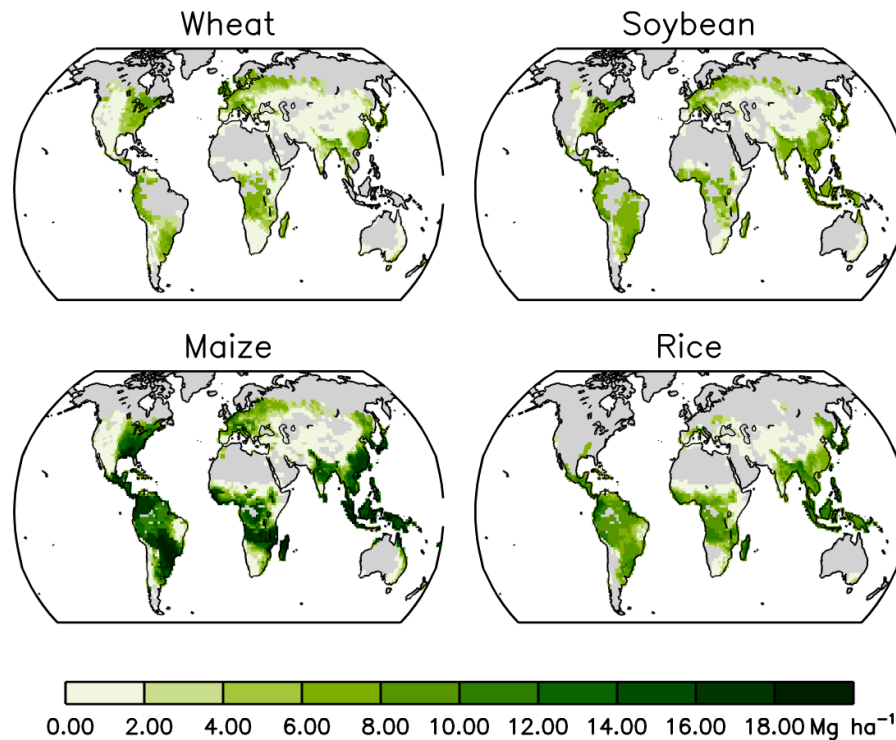Full Screen / Esc

Printer-friendly Version

Interactive Discussion

Full Screen / Esc

Printer-friendly Version

Interactive Discussion

Figure 1. Schematic of JULES-crop.

Figure 2. Fraction of daily accumulated net primary productivity partitioned to roots (purple), stems (blue), leaves (yellow) and harvested parts (red) of the crop as a function of development index (DVI; 0 = emergence, 1 = flowering, 2 = maturity) for wheat, rice, soy bean and maize.
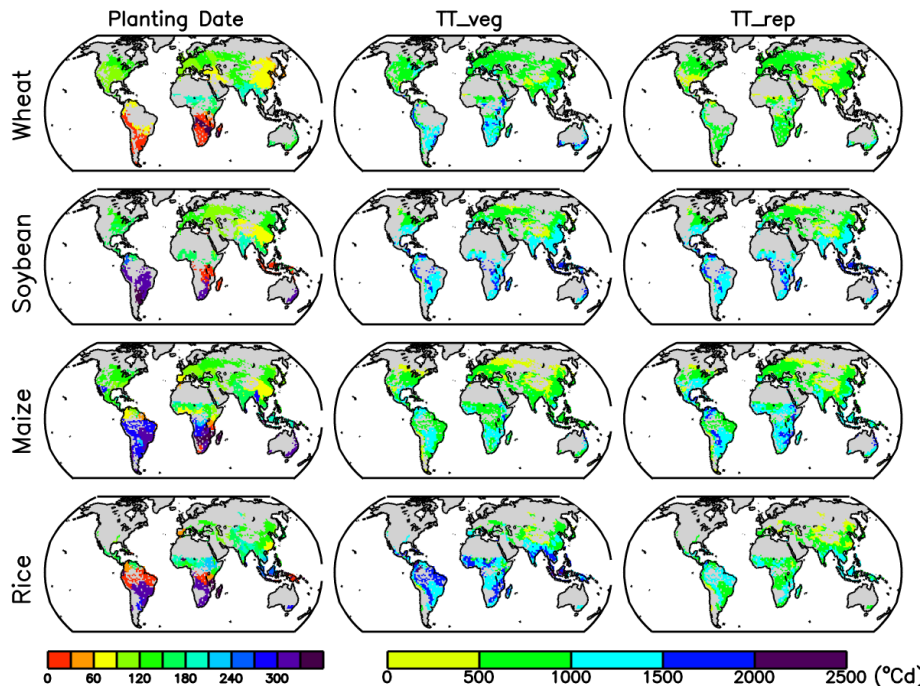
Figure 3. Global distribution planting date from Sacks et al. (2010), interpolated to NCEP grid, and the thermal time from emergence to flowering (TT_veg) and from flowering to harvest (TT_rep) for each crop type. See text for details of calculation.

Title Page

Abstract | Introduction

Conclusions | References

Tables | Figures

|◄ | ►|

◄ | ►

Back | Close

Full Screen / Esc

Printer-friendly Version

Interactive Discussion

Figure 4. Global distribution of average wheat, soy bean, maize and rice yield assuming a moisture content of 16 % and a carbon fraction of 0.5.

Title Page

Abstract | Introduction

Conclusions | References

Tables | Figures

|◄ | ►|

◄ | ►

Back | Close

Full Screen / Esc

Printer-friendly Version

Interactive Discussion
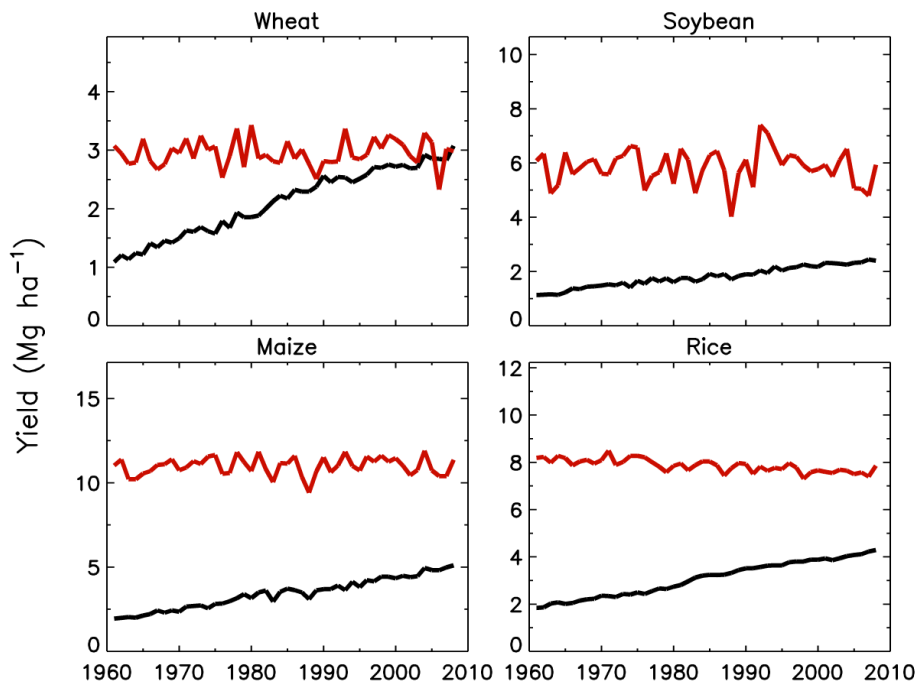
Figure 5. Simulated (red) and observed (black) global yield of wheat, soy bean, maize and rice between 1961–2008.

Title Page

Abstract · Introduction

Conclusions · References

Tables · Figures

|◄ · ►|

◄ · ►

Back · Close

Full Screen / Esc

Printer-friendly Version

Interactive Discussion
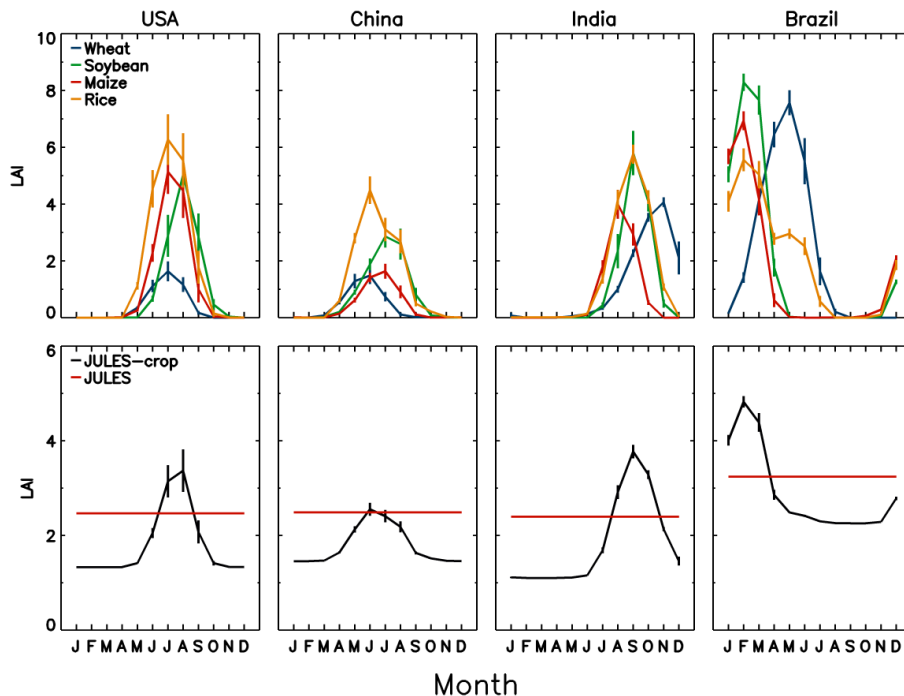
Figure 6. Country crop area weighted annual cycle of crop typ (top) and grid-box mean (bottom) leaf area index (LAI). Area averages weighted by crop area in top panels, and total plant functional type area in bottom panesl. Vertical bars indicate standard deviation of monthly values.

Full Screen / Esc
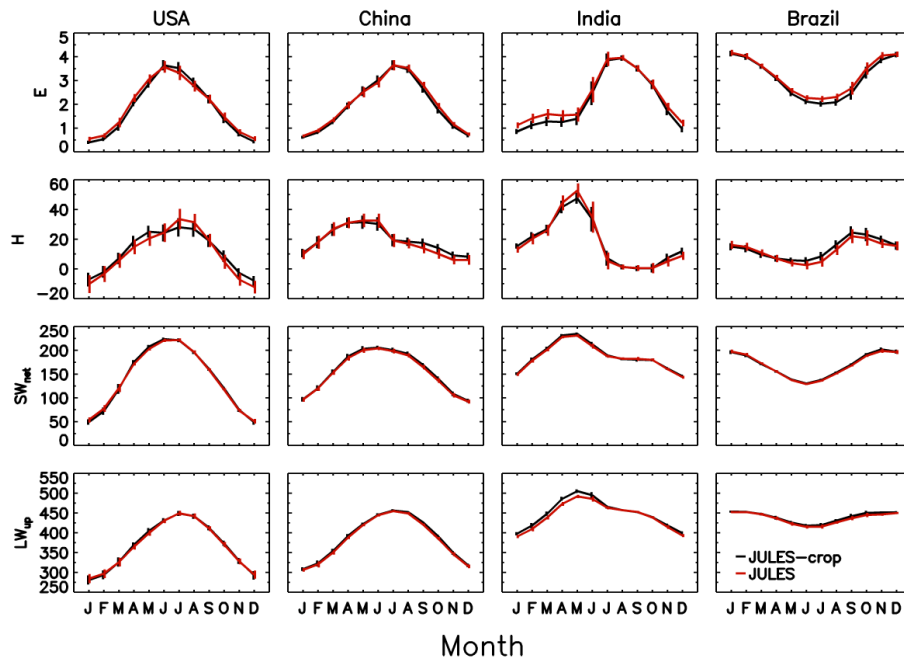
Figure 7. Country crop area weighted average mean annual cycle of surface moisture flux (E), sensible heat flux (H), net short wave radiation (SW_{net}) and upward long wave radiation (LW_{up}) from JULES-crop simulation (red) and standard JULES simulation (black) forced with CRU-NCEP meteorological driving data. Vertical bars indicate standard deviation of monthly values.
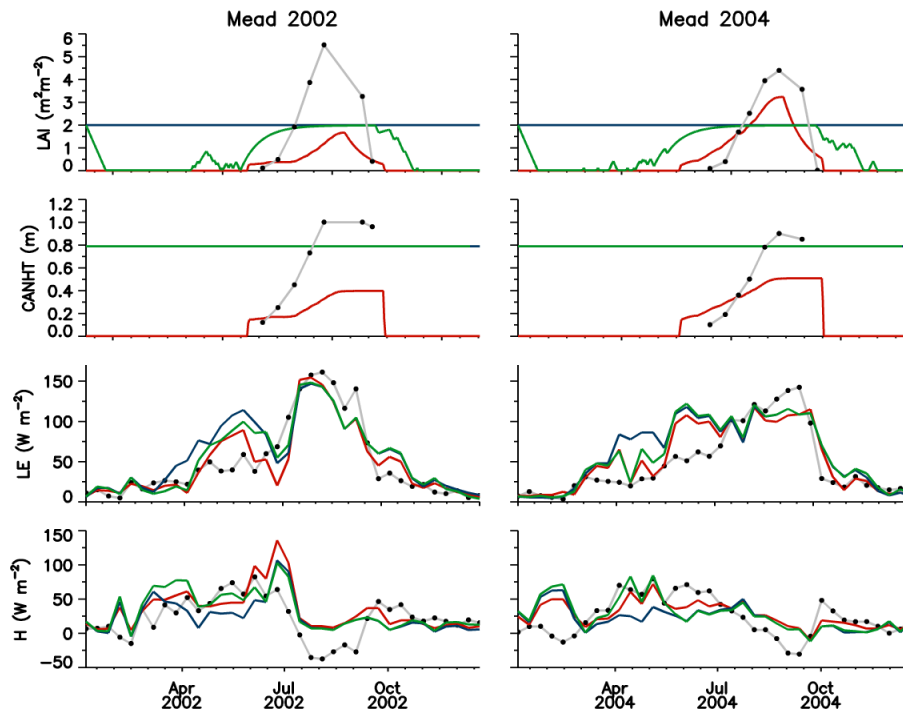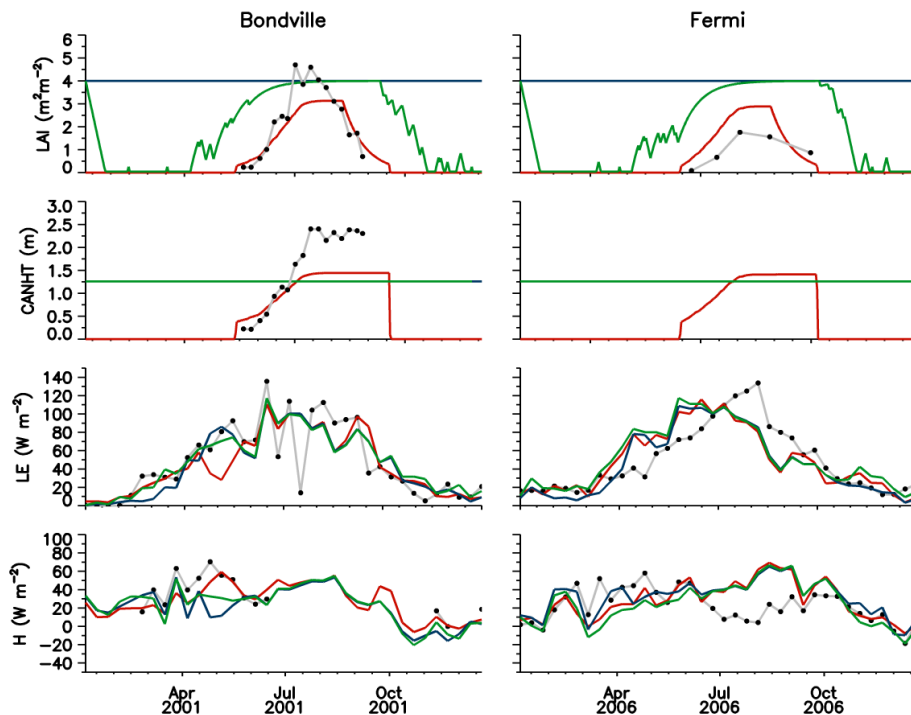
Figure 8. Simulated (solid lines) and observed (dots) leaf area index, canopy height, latent and sensible heat fluxes for Mead FLUXNET Site 2 in 2002 (left) and 2004 (right). Simulations performed with JULES-crop crop type soy bean (red), standard JULES C3 grass plant functional type with phenology (green), and standard JULES C3 grass plant functional type without phenology (blue).

Discussion Paper | Discussion Paper | Discussion Paper | Discussion Paper

GMDD

7, 6773–6809, 2014

JULES-crop

T. Osborne et al.

Title Page

Abstract | Introduction

Conclusions | References

Tables | Figures

|◄ | ►|

◄ | ►

Back | Close

Full Screen / Esc

Figure 9. Simulated (solid lines) and observed (dots) leaf area index, canopy height, latent and sensible heat fluxes for FLUXNET site Bondville in 2001 and Fermi in 2006. Simulations performed with JULES-crop crop type maize (red), standard JULES C4 grass plant functional type with phenology (green), and standard JULES C4 grass plant functional type without phenology (blue).

Discussion Paper | Discussion Paper | Discussion Paper | Discussion Paper |

GMDD

7, 6773–6809, 2014

JULES-crop

T. Osborne et al.

Title Page

Abstract · Introduction

Conclusions · References

Tables · Figures

⏮ · ⏭

◀ · ▶

Back · Close

Full Screen / Esc

Printer-friendly Version

Interactive Discussion